

# NLO QCD corrections to excited lepton production at the LHC

Swapan Majhi<sup>\*†</sup>

*Department of Theoretical Physics,  
Indian Association for the Cultivation of Science  
Kolkata 700032 India.*

## Abstract

We revisited excited leptons ( $\bar{l}^*l$ ) production through gauge mediation only at LHC, followed by their two body decays into Standard Model (SM) particles. We include the next-to-leading order (NLO) QCD corrections to these processes. We have shown that these corrections can be substantial and significant. We also show that the scale dependence of the NLO cross section is greatly reduced as compare to leading order (LO) cross section.

---

<sup>\*</sup>E-mails: tpskm@iacs.res.in

<sup>†</sup>Work supported by CSIR Pool Scheme (Pool No. 8545-A)

# 1 Introduction

In the recent years in particle phenomenology, a lot of attention goes into find the suitable model beyond the standard model (BSM) physics, which can explain many issues like the replication of the fermion families, dark matter, baryogenesis etc. that are still not understood within the framework of the Standard Model (SM). The quark-lepton composite model [1] is one of the prime candidate among others like supersymmetry [2], grand unification [3, 4] (with or without supersymmetry), family symmetries (gauged or otherwise).

The replication of fermion generations suggests the possibility of quark-lepton compositeness. In these theories [5, 6], the fundamental constituents, *preons* [7], experience an additional strong and confining force. At energies far above a certain (compositeness) scale ( $\Lambda$ ), preons are almost free. Below this scale  $\Lambda$ , the interaction of preons become very strong forcing them to form a bound state of quarks and leptons. Understandably, in such models, higher (excited) states of quarks ( $q^*$ ) and leptons ( $l^*$ ) must also exist.

Since the composite fermion is just an excited state of the SM fermion, generalized dipole moment-like terms should mediate interactions between them. The corresponding effective Lagrangian [8] is given by

$$\mathcal{L}_{GM} = \frac{1}{2\Lambda} \bar{f}_R^* \sigma^{\mu\nu} \left[ g_s f_s \frac{\lambda^a}{2} G_{\mu\nu}^a + g f'' \frac{\tau}{2} \cdot W_{\mu\nu} + g' f' \frac{Y}{2} B_{\mu\nu} \right] f_L + h.c. \quad (1)$$

where  $G_{\mu\nu}^a$ ,  $W_{\mu\nu}$  and  $B_{\mu\nu}$  are the field strength tensor of the  $SU(3)$ , the  $SU(2)$  and the  $U(1)$  gauge fields respectively.  $f^*$  and  $f$  denote the excited fermion and SM fermion respectively.  $f_s$ ,  $f''$  and  $f'$  are the parameters of the compositeness. Usually they are taken to be order of 1.

In the absence of a full theory, all the interactions of such composite fermions cannot be written down unambiguously. Rather, one must take recourse to an effective Lagrangian. The latter, typically, would contain not only the term of eqn.(1) above but others as well. The corresponding Wilson coefficients can only be determined if the ultraviolet completion was well-known and are, a priori, unknown within the context of the effective theory. The literature abounds with the discussion of one such subset of operators, namely four-fermion interactions between a pair of SM fermions and a pair of composites (the so-called contact interaction [9]). It should be realized that such operators are suppressed by an additional power of  $\Lambda$  as compared to the terms of eqn.(1). Thus, it makes eminent sense to consider the above while neglecting the four-fermion terms.

It is evident that these operators may lead to significant phenomenological effects in collider experiments, like  $e^+e^-$  [10],  $eP$  [11] or hadronic [12–14]. It is quite obvious that the effects would be more pronounced at higher energies, given the higher-dimensional nature of  $\mathcal{L}_{GM}$ . The best low-energy bounds on such composite operator would arise from the precise measurement of leptonic branching ratios (BR) of lepton  $\tau$  [15]. The loop effect of these excited states can modify the SM branching ratio predictions and comparison with the experimental data can impose bounds on masses of these new particles and their couplings. These bounds are quite weak [16]. The constraints on such excited states came from the Delphi [10] and CDF [12] experiments. More recently, the measurement of the  $\bar{l}l\gamma$  cross section [13, 14] at high invariant masses sets the most stringent limits on contact interactions.

It is a well known fact that the QCD corrections can alter the cross sections quite significantly at hadron colliders. Recently, the production of  $\bar{l}^*l(\bar{l}l\gamma)$  in the context of contact interactions have received much attention from both CMS [13] and ATLAS [14] collaborations. They have searched for heavy excited lepton via  $\bar{l}l\gamma$  channel and put the mass bound on excited lepton at



affect only hadronic currents with leptonic current being a mute spectator, the offending higher dimensional nature of the effective Lagrangian never comes into play in our calculations. Therefore it is convenient to express our matrix element for the process as a sum of several current-current pieces with a “propagator” in between. In other words, symbolically,

$$\mathcal{M}^{\text{Total}} = \sum_j \mathcal{J}_j^{\text{Had}} \cdot P_j \cdot \mathcal{J}_j^{\text{Lept}} \quad (5)$$

where the dots  $(\cdot)$  denote Lorentz index contractions as appropriate and the propagators  $P_j$  are

$$P_\gamma = \frac{i}{Q^2} g_{\mu\nu} \equiv g_{\mu\nu} \tilde{P}_\gamma \quad P_Z = \frac{i g_{\mu\nu}}{Q^2 - M_Z^2 - i M_Z \Gamma_Z} \equiv g_{\mu\nu} \tilde{P}_Z. \quad (6)$$

With this definition, the hadronic cross section can be written as

$$2S \frac{d\sigma^{P_1 P_2}}{dQ^2}(\tau, Q^2) = \frac{1}{2\pi} \sum_{j, j'=\gamma, Z} \tilde{P}_j(Q^2) \tilde{P}_{j'}^*(Q^2) \mathcal{L}_{jj'}(Q^2) W_{jj'}^{P_1 P_2}(\tau, Q^2) \quad (7)$$

where the hadronic structure function  $W$  is defined to be

$$W_{jj'}^{P_1 P_2}(\tau, Q^2) = \sum_{a, b, j, j'} \int_0^1 dx_1 \int_0^1 dx_2 f_a^{P_1}(x_1) f_b^{P_2}(x_2) \int_0^1 dz \delta(\tau - zx_1 x_2) \bar{\Delta}_{ab}^{jj'}(z, Q^2, \epsilon). \quad (8)$$

Note that, the bare partonic coefficient function  $\bar{\Delta}$  contains all the singularities, namely, ultraviolet, soft and collinear divergences. To handle these, we have followed the dimensional regularization ( $DR$ ) scheme. The renormalization of  $VA$ -type interactions is quite established (see for example, in Ref. [20]). After the renormalization, one must get the ultraviolet regularized (and renormalized) expressions. To the ultraviolet regularized expressions, we must add the contribution from the real gluon emission processes (bremsstrahlung) as well as the Compton processes (gluon initiated processes). In this way, we remove the soft singularities and the left over expressions contain only collinear singularities. These collinear singularities can be removed through mass factorization. Finally one gets the finite coefficient function  $\Delta$  as in eqn(12).

The leptonic tensor is given by

$$\mathcal{L}^{jj' \rightarrow ll'} = \int \prod_i^2 \left( \frac{d^n l_i}{(2\pi)^n} 2\pi \delta^+(l_i^2) \right) (2\pi)^n \delta^{(n)}(q - l_1 - l_2) |\mathcal{M}^{jj' \rightarrow l^+ l^-}|^2, \quad (9)$$

which leads to

$$\mathcal{L}_{jj' \rightarrow ll'} = \left( -g_{\mu\nu} + \frac{q_\mu q_\nu}{Q^2} \right) \mathcal{L}_{jj'}(Q^2) \quad (j, j' = \gamma, Z) \quad (10)$$

with

$$\begin{aligned} \mathcal{L}_{\gamma\gamma}(Q^2) &= \frac{\alpha}{6\Lambda^2} |f_\gamma|^2 Q^2 \mathcal{L}(Q^2) & \mathcal{L}_{ZZ}(Q^2) &= \frac{\alpha}{6\Lambda^2} |f_Z|^2 Q^2 \mathcal{L}(Q^2) \\ \mathcal{L}_{\gamma Z}(Q^2) &= \frac{\alpha}{3\Lambda^2} f_Z f_\gamma Q^2 \mathcal{L}(Q^2) & \mathcal{L}(Q^2) &= Q^2 + m_1^2 + m_2^2 - \frac{2}{Q^2} (m_1^2 - m_2^2)^2 \end{aligned} \quad (11)$$

The physical hadronic cross section can be obtained by convoluting the finite coefficient functions with appropriate parton distribution functions and hence the inclusive differential cross section is given by

$$\begin{aligned}
2S \frac{d\sigma^{P_1 P_2}}{dQ^2}(\tau, Q^2) &= \sum_q \int_0^1 dx_1 \int_0^1 dx_2 \int_0^1 dz \delta(\tau - zx_1 x_2) \mathcal{F}_q^{VA} \mathcal{G}_{VA} \\
\mathcal{G}_{VA} &\equiv H_{q\bar{q}}(x_1, x_2, \mu_F^2) \left\{ \Delta_{q\bar{q}}^{(0),VA}(z, Q^2, \mu_F^2) + a_s \Delta_{q\bar{q}}^{(1),VA}(z, Q^2, \mu_F^2) \right\} \\
&+ \left\{ H_{qg}(x_1, x_2, \mu_F^2) + H_{gq}(x_1, x_2, \mu_F^2) \right\} a_s \Delta_{qg}^{(1),VA}(z, \mu_F^2),
\end{aligned} \tag{12}$$

where the renormalized parton flux  $H_{ab}(x_1, x_2, \mu_F^2)$  and the finite coefficient functions  $\Delta_{ab}^{(i)}$  are given in Refs. [18–20]. The constant  $\mathcal{F}^{VA}$  contains information of all the couplings, propagators and the massive final state particles which is given by

$$\begin{aligned}
\mathcal{F}_q^{VA} &= \frac{2\alpha^2}{3} \frac{\beta}{\Lambda^2} \mathcal{L}(Q^2) \left[ |f_\gamma|^2 \frac{e_q^2}{Q^2} - e_q f_\gamma f_Z (g_q^L + g_q^R) \frac{(Q^2 - m_Z^2)}{Q^2} Z_Q \right. \\
&\quad \left. + \frac{1}{2} |f_Z|^2 ((g_q^L)^2 + (g_q^R)^2) Z_Q \right],
\end{aligned} \tag{13}$$

$$\begin{aligned}
Z_Q &= \frac{Q^2}{(Q^2 - m_Z^2)^2 + \Gamma_Z^2 m_Z^2} & g_q^R &= -2T_q^3 \csc \theta_W - e_q \tan \theta_W \\
g_q^L &= -e_q \tan \theta_W & \beta &= \left( 1 + \frac{m_1^4}{Q^4} + \frac{m_2^4}{Q^4} - 2\frac{m_1^2}{Q^2} - 2\frac{m_2^2}{Q^2} - 2\frac{m_1^2 m_2^2}{Q^2} \right)^{\frac{1}{2}}.
\end{aligned} \tag{14}$$

### 3 Results and Discussion

In the previous section, we have calculated the differential distributions with respect to invariant mass ( $Q$ ) of  $\bar{l}^* l$  (one excited lepton and SM lepton). For our interest, we have expressed the above differential distribution (eqn.(12)) to the total cross section by integrating over  $Q^2$  and it is given by

$$\sigma^{P_1 P_2}(M_*^2, S, \Lambda) = \int \frac{d\sigma^{P_1 P_2}(\tau, Q^2)}{dQ^2} dQ^2. \tag{15}$$

In our numerical analysis, we present our results at three different LHC energies  $\sqrt{S} = 13, 33, 100$  TeV for the simplest case where the factorization ( $\mu_F$ ) and renormalization scale ( $\mu_R$ ) considered to be equal to the invariant mass ( $Q$ ) of  $\bar{l}^* l$ . Later, we have shown the scale dependence of our results by introducing the factorization scale,  $\mu_F^2 (\mu_R^2) \neq Q^2$ . Since the QCD correction does not depend on the contact interaction scale  $\Lambda$ , for definiteness we have used a particular value of  $\Lambda = 2, 6$  TeV for each LHC energy unless it is quoted. Through out our numerical analysis, we have used Cteq6Pdf [21] and MSTW 2008 [22] parton distribution functions (PDFs) otherwise mentioned specifically.

We will first discuss the NLO corrections of  $\bar{l}^* l$  (and  $\bar{l} l^*$  as well) productions in general and later we consider only a particular process  $\bar{l} l \gamma$  production. This particular process has been analyzed by both CMS [13] and ATLAS [14] in the context of contact interaction at low center of mass energy ( $\sqrt{S} = 7$  TeV). Since the production cross section of  $\bar{l}^* l$  through gauge mediation at this center of mass energy ( $\sqrt{S} = 7$  TeV) is quite small, they did not open up this

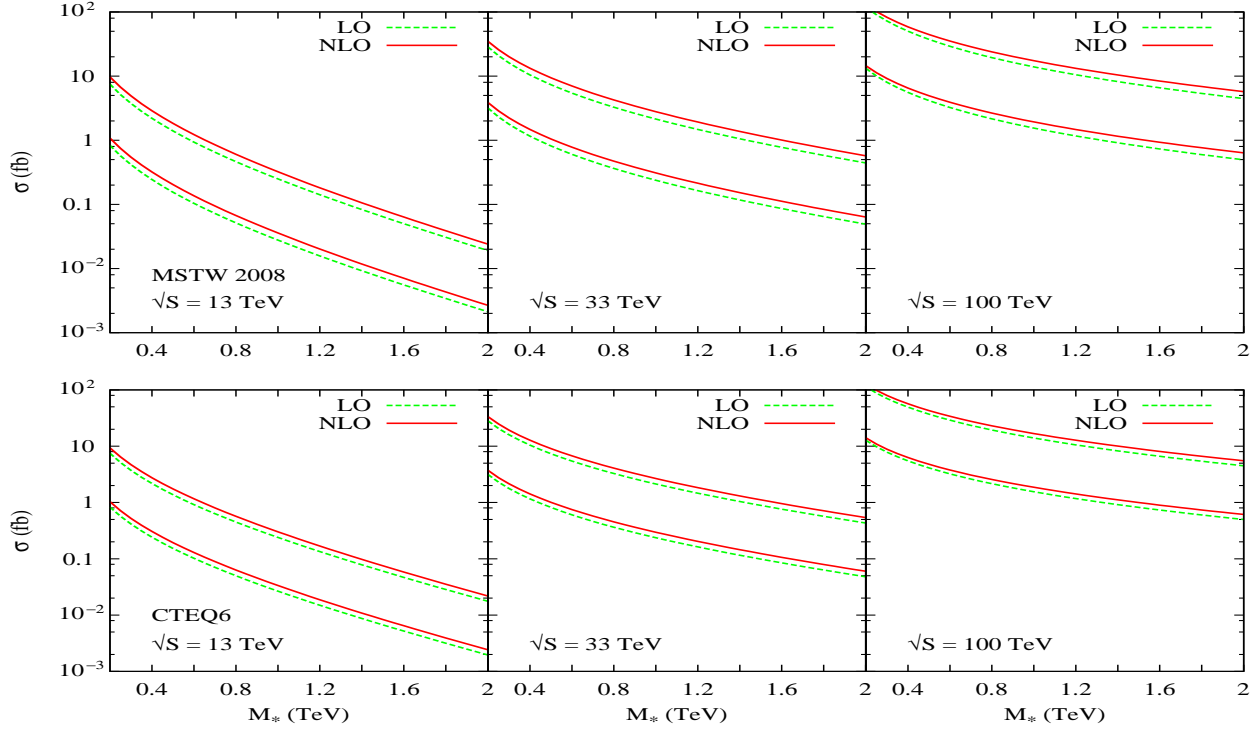


Figure 1: Variation of total cross-section for  $\bar{l}^*l$  production with respect to excited lepton mass ( $M_*$ ) at the LHC. Upper (lower) set represents for  $\Lambda = 2(6)$  TeV.

channel. However at higher LHC energies ( $\sqrt{S} = 13, 33$  TeV and/or 100 TeV), this particular process may play an important role for searching the excited lepton in the beyond standard model scenario. The above mentioned particular process attains through two body decaying process of excited lepton ( $l^*$ ). The two body decay of excited lepton does not have any effect on QCD correction thus the NLO QCD correction to the  $\bar{l}l\gamma$  production process is same as NLO QCD correction to the  $\bar{l}^*l$  as described in the next section 3.1.

In figure 1, we have plotted the total cross section of ( $\bar{l}^*l$ ) as a function of excited lepton mass ( $M_*$ ). The cross sections presented in figure 1 contain the contributions of all the light flavors ( $u, d, s$ -quarks) as those for heavier flavor being essentially negligibly small. As we have seen from figure 1 that the cross section decreases with excited lepton mass ( $M_*$ ) due to not only the fall of partonic cross section but also due to the fall in parton distribution functions (and hence effective flux of  $q\bar{q}$  as well as  $qg$ ) at higher momentum fraction ( $\tau$  and hence Bjorken scale  $x$ ). The fall of the total cross section is more at lower center of mass (c.o.m.) energies than the higher c.o.m. energy. At higher momentum fraction  $\tau$ , we are integrating over small phase space region at low center of mass energy  $\sqrt{S}$ .

To quantify the enhancement of NLO cross section, we define a variable called  $K$ -factor as given by

$$K = \frac{\sigma^{NLO}}{\sigma^{LO}} \quad (16)$$

where the LO (NLO) cross sections are computed by convoluting the corresponding parton-level cross sections with the LO (NLO) parton distribution functions.

In figure (2) we have shown the variation of  $K$ -factor with respect to the excited lepton mass ( $M_*$ ). The variation of the total  $K$ -factor is about 25% – 30% for c.o.m energies  $\sqrt{S} = 13, 33$

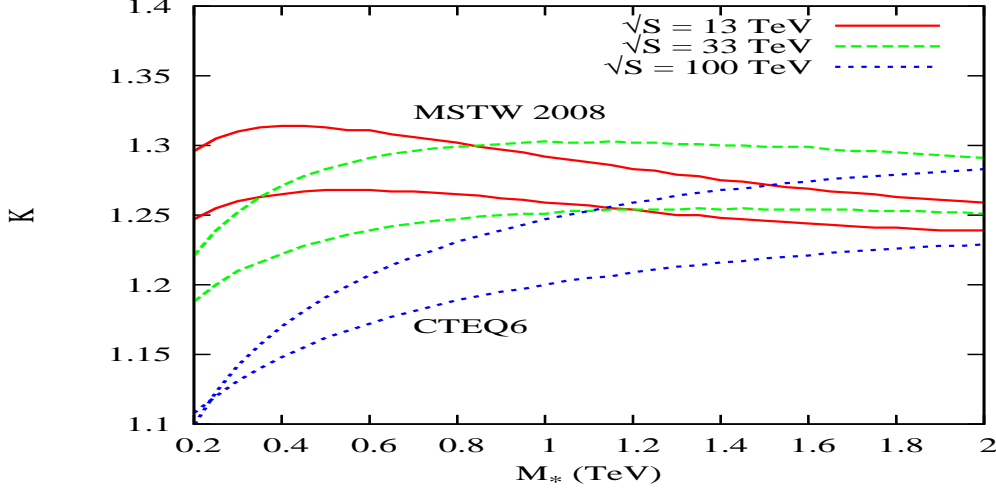


Figure 2: Variation of  $K$ -factor with respect to the excited lepton mass ( $M_*$ ) for  $\Lambda = 2$  TeV at the LHC for  $\bar{l}^*l$  channel. Upper (lower) set is for MSTW 2008 (CTEQ6) PDFs.

TeV. For much higher c.o.m energy  $\sqrt{S} = 100$  TeV, the variation of the total  $K$ -factor is about 10%–25% for  $M_* \leq 1$  TeV and increases very fast. For  $M_* \geq 1$  TeV, the  $K$ -factor increases slowly with  $M_*$  (20%–30%). In figures (2), the rate of fall of the  $K$ -factor is much slower at lower c.o.m energy (say  $\sqrt{S} = 13, 33$  TeV) than the higher c.o.m energy  $\sqrt{S} = 100$  TeV. At lower c.o.m energy (higher momentum fraction,  $0.00024 \leq \tau \leq 0.024$  for  $\sqrt{S} = 13$  and hence the Bjorken  $x$ ), we are integrating relatively smaller phase space region. As excited lepton mass increases, the variation of  $K$ -factor becomes smooth due to the fact that the valence quark (mostly  $u$  and  $d$ -quark) distributions dominate over sea quark and gluon distributions. At higher c.o.m energy (lower momentum fraction,  $0.000004 \leq \tau \leq 0.00004$  for  $\sqrt{S} = 100$  TeV), we are integrating over relatively larger phase space. In this region, the sea ( $s$ ) quark and gluon ( $g$ ) distributions dominate over the valence quark ( $u$  and  $d$ -quark) distributions. Therefore the compton-like subprocess (in particular,  $g s(\bar{s}) \rightarrow \bar{l}^* l s(\bar{s})$ ) dominates due to large gluon ( $g$ ) and sea-quark fluxes and hence explains such behavior of  $K$ -factor.

### 3.1 $\bar{l}l\gamma$ production

The decaying of heavy excited lepton into a light SM lepton and a electroweak gauge bosons  $V(\equiv \gamma, Z, W)$  according to the Lagrangian(1) produce a particular process ( $\bar{l}l\gamma$ ) of our prime interest. Therefore the total NLO cross section of lepton pair ( $\bar{l}l$ ) and a gauge boson  $V$  can be calculated by multiplying the branching ratio to the eqn.(15) as given below

$$\sigma^{P_1 P_2}(M_*, S, \Lambda) = BR(l^* \rightarrow lV) \int \frac{d\sigma^{P_1 P_2}(\tau, Q^2)}{dQ^2} dQ^2. \quad (17)$$

The partial decay width of excited lepton for various electroweak gauge bosons is given by

$$\Gamma(l^* \rightarrow lV) = \frac{1}{8} \alpha f_V^2 \frac{M_*^2}{\Lambda^2} \left(1 - \frac{m_V^2}{M_*^2}\right) \left(2 + \frac{m_V^2}{M_*^2}\right), \quad (18)$$

with

$$f_\gamma = f T_3 + f' \frac{Y}{2}, \quad (19)$$

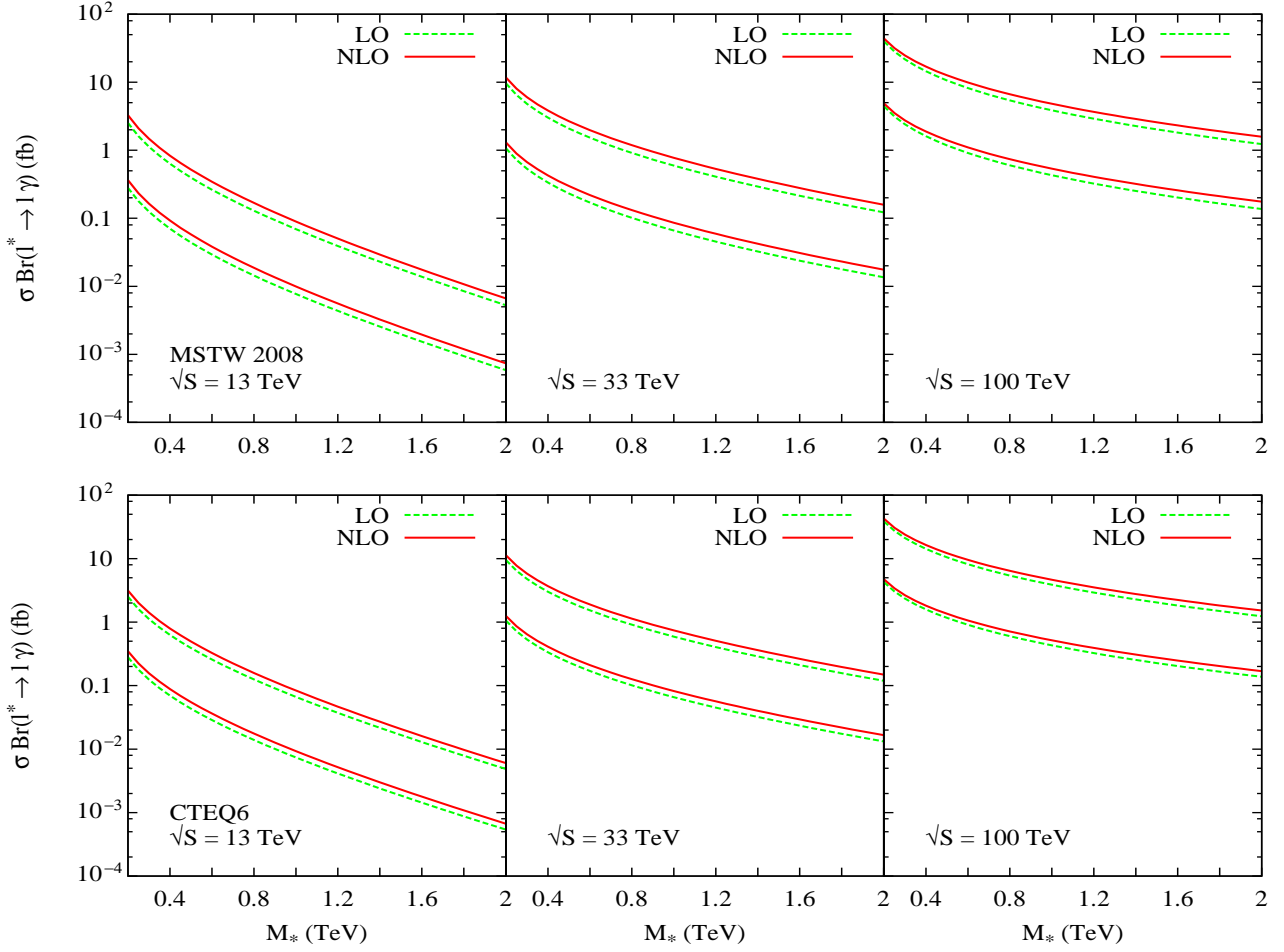


Figure 3: Total cross-section for  $\bar{l}l\gamma$  production at the LHC. For each set, the solid (dashed) lines refer to NLO (LO) cross sections. Upper (lower) set is for  $\Lambda = 2(6)$  TeV.

$$f_Z = f T_3 \cot \theta_W - f' \frac{Y}{2} \tan \theta_W, \quad (20)$$

$$f_W = \frac{f}{\sqrt{2}} \csc \theta_W, \quad (21)$$

where  $T_3$  denotes the third component of the weak isospin and  $Y$  represents the weak hypercharge of excited lepton.  $\theta_W$  is the Weinberg's angle. The compositeness parameters  $f$  and  $f'$  are taken to be unity through out our analysis. The variation of these parameters have been considered in elsewhere (for example in the Refs. [23, 24]). The details of decay width and branching fraction of excited lepton is given in [17] (see table 1 and references therein).

In figure 3, we have plotted the total cross section versus invariant mass  $M_*(\equiv M_{l\gamma})$  of one SM lepton( $l$ ) and a photon ( $\gamma$ ). We have shown for two different PDFs, namely, CTEQ6 [21] and MSTW 2008 [22]. As explain before, the cross section decreases in increase of invariant mass  $M_*$ . The variation of the cross section looks same for two different PDFs, actually they are not. This can be found out from figure 5 and has been explained later on. From the figure 3, we see that as the composite scale ( $\Lambda$ ) increases, the cross section (both LO as well as NLO) decreases uniformly as  $\Lambda^{-2}$  as expected (from eqn.(1)) for a fixed center of mass energy ( $\sqrt{S}$ ) and for different values of  $\Lambda$ , the cross section scales accordingly. Therefore, one can obtain the cross section (for both LO as well as NLO) for arbitrary values of  $\Lambda$  by multiplying with an appropriate scale factor to our results.



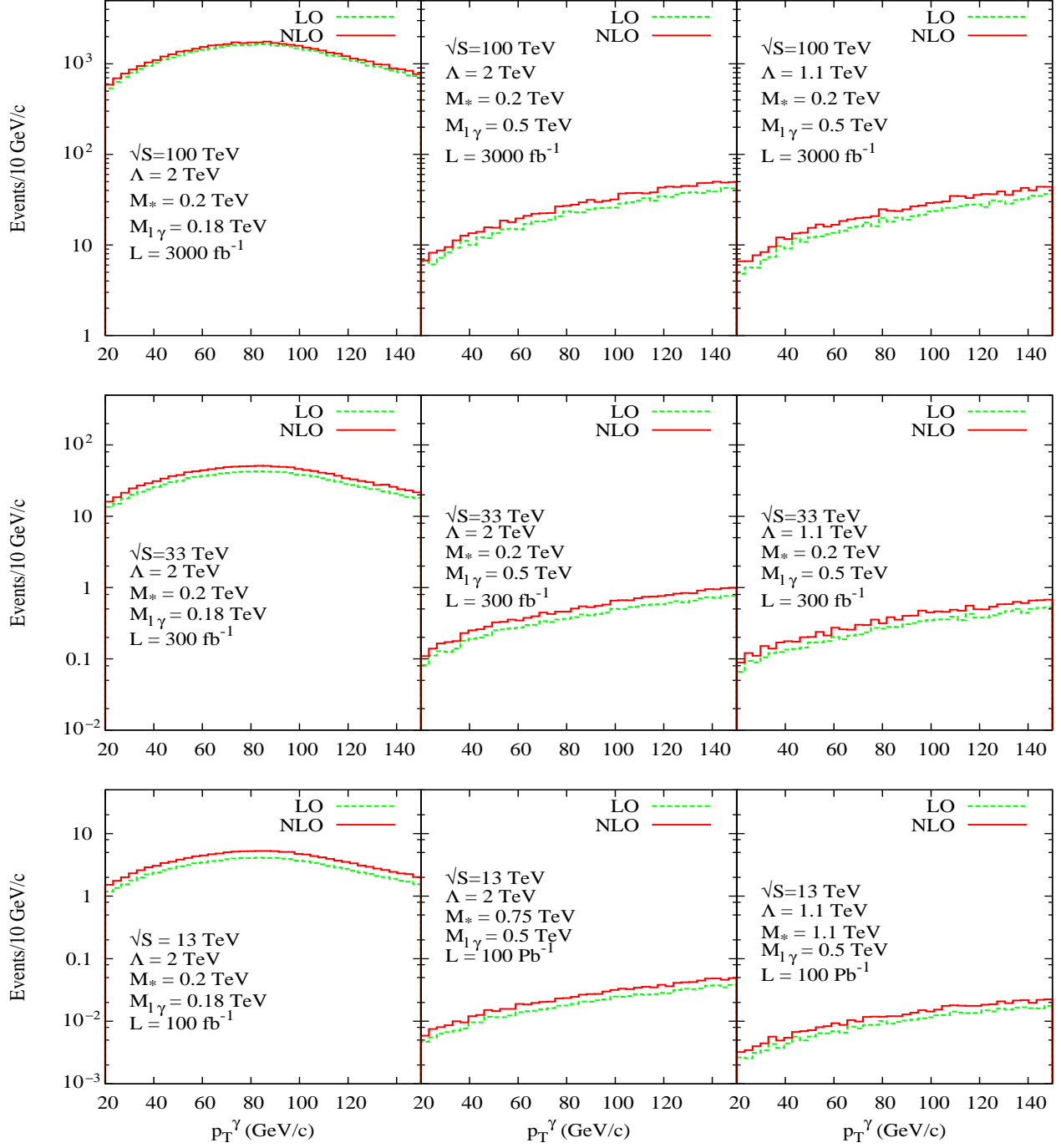


Figure 4: *Photon transverse momentum distributions at three different excited lepton masses and three different LHC energies for MSTW 2008 parton distribution functions.*

In figures 4, we have displayed the photon transverse momentum distribution. In this case, we use with same lepton-photon invariant mass cut ( $M_{l\gamma}^{cut}$ ) as given in [13]. We have considered the projected luminosity 100, 300 (3000)  $fb^{-1}$  at  $\sqrt{S} = 13, 33 (100)$  TeV LHC energies respectively. From the figures, one can see that the production rates are increased by including NLO QCD corrections.

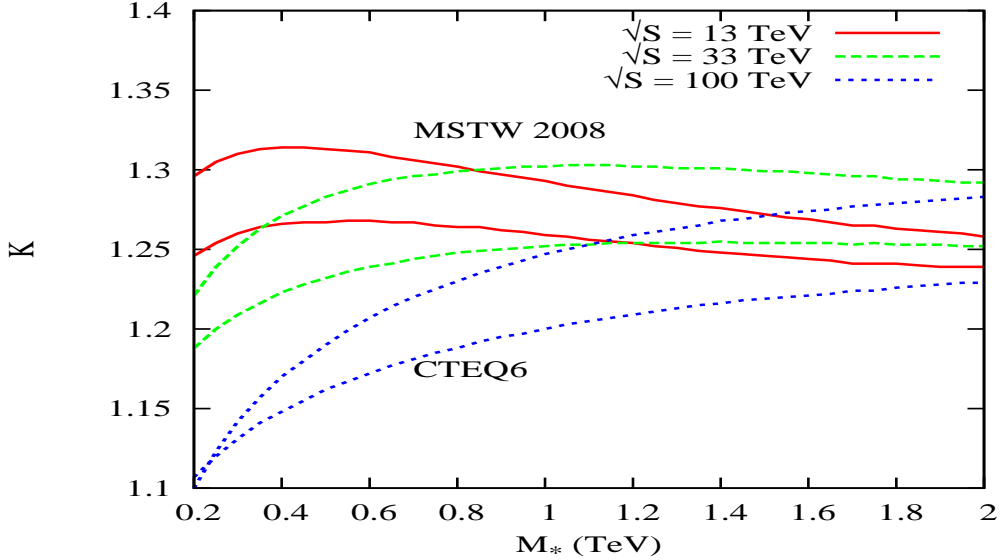


Figure 5:  $K$ -factor for  $\bar{l}l\gamma$  production at three different LHC energies. Upper (lower) set is for MSTW 2008 (CTEQ6) PDFs.

We have shown the variation of total  $K$ -factor with respect to the  $M_*$  in figure 5. The variation of  $K$ -factor is very similar to the figure 2 as expected and hence it has been explained there itself. The very wide range of  $K$ -factor difference between the two PDFs, namely, CTEQ6 and MSTW 2008 is due to their different parameterizations of their parton distribution functions (owing to their use of different data sets to extract the PDFs).

### 3.2 The choice of Scale

In our above discussions, we have considered the factorization scale,  $\mu_F$ , (relevant to both LO and NLO) and the renormalization scale,  $\mu_R$ , (relevant only to NLO) to be same as the invariant mass ( $Q$ ) of  $\bar{l}^*l$ . However the cross section depends only on physical scales like the c.o.m. energy ( $\sqrt{S}$ ) and the masses of final state particles ( $M_*$ ). Since there is no theoretical guideline to choose a particular scale choice the abovementioned scale choice is completely arbitrary. Now we can check the scale dependence of our result by introducing another scale called factorization scale  $\mu_F^2 (= \mu_R^2$  the renormalization scale, for simplicity). To quantify the scale dependence if we define a ratio  $R$ ,

$$R^I = \frac{\sigma^I(S, M_*, \mu_F^2)}{\sigma^I(S, \mu_F^2 = M_*^2)}, \quad I = LO, NLO, \quad (22)$$

the ratio  $R$  close to unity signify low sensitivity to scale choice and hence a more robust result.

In figure 6, we have shown the variation of the cross section with respect to the excited lepton mass at different the factorization scale. From the figure 6, it is clear that the scale dependence reduces greatly at NLO cross section compare to LO cross section. This signifies the necessity

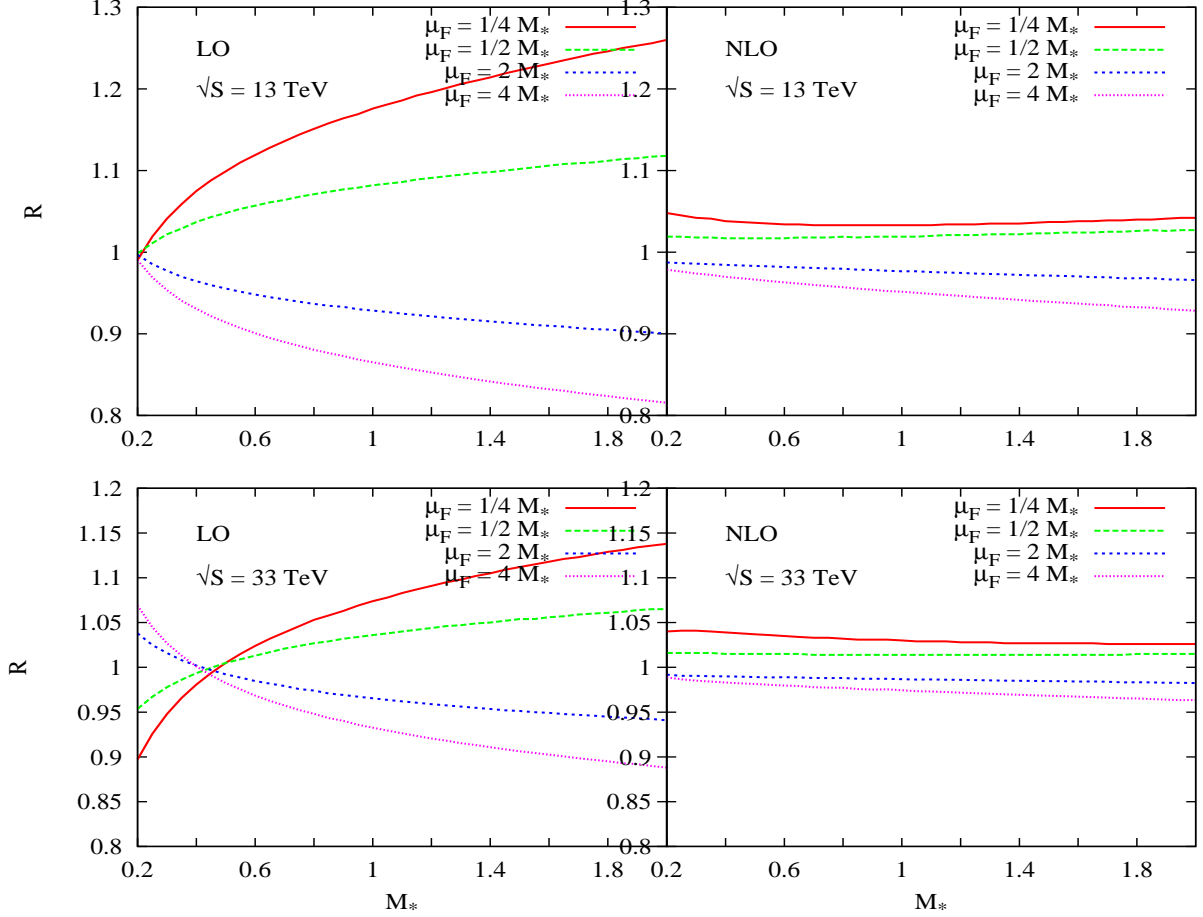


Figure 6: Variation of the ratio,  $R$  (defined in eqn.(22)) with respect to the excited lepton mass ( $M_*$ ) at different factorization scale  $\mu_F$  using CTEQ6 PDFs.

of NLO QCD corrections. The remaining very small scale ambiguity can be reduced by adding still higher order corrections.

## 4 Conclusions

In conclusion, we have systematically performed the next-to-leading order QCD corrections for the chromomagnetic type interactions as given in eqn.(1). As opposed to naive expectations, we have showed that the QCD corrections are meaningful and reliable to such non-renormalizable theory.

We have analyzed the variation of cross section with respect to the excited lepton mass (and hence the invariant mass of one SM lepton and a SM gauge boson) at the LHC. The enhancement of NLO cross section over the LO cross section is found to be quite significant. To quantify the enhancement, we present the corresponding  $K$ -factors in a suitable form for experimental analysis. We have also showed the scale dependence of our results. As expected, we have seen that the scale dependences reduce greatly for the NLO results as compared to that for the LO case.

# Acknowledgments

Author would like to thank Debajyoti Choudhury for useful discussions and comments.

# References

- [1] E. Eichten, K.D. Lane and M.E. Peskin, Phys. Rev. Lett. **50** (1983) 811 ;  
E. Eichten, I. Hinchliffe, K.D. Lane and C. Quigg, Rev. Mod. Phys. **56** (1984) 579.
- [2] H. P. Nilles, Phys. Rept. **110** (1984) 1;  
H. E. Haber and G. L. Kane, Phys. Rept. **117** (1985) 75;  
*Perspectives in Supersymmetry*, ed. G.L. Kane, World Scientific (1998);  
*Theory and Phenomenology of Sparticles*: M. Drees, R.M. Godbole and P. Roy, World Scientific (2005).
- [3] J. C. Pati and A. Salam, Phys. Rev. D **10** (1974) 275.
- [4] H. Georgi and S. L. Glashow, Phys. Rev. Lett. **32** (1974) 438 ;  
P. Langacker, Phys. Rept. **72** (1981) 185.
- [5] Jogesh C. Pati, Abdus Salam and J.A. Strathdee Phys.Lett. **B59** (1975) 265;  
H. Fritzsch and G. Mandelbaum, Phys.Lett. **B102** (1981) 319;  
W. Buchmuller, R.D. Peccei and T. Yanagida, Phys.Lett. **B124** (1983) 67;  
Nucl.Phys.**B227** (1983) 503; Nucl.Phys.**B237** (1984) 53;  
U. Baur and H. Fritzsch, Phys.Lett. **B134** (1984) 105;  
Xiaoyuan Li and R.E. Marshak, Nucl.Phys.**B268** (1986) 383;  
I. Bars, J.F. Gunion and M. Kwan Nucl.Phys.**B269** (1986) 421;  
G. Domokos and S. Kovesi-Domokos, Phys.Lett.**B266** (1991) 87;  
Jonathan L. Rosner and Davison E. Soper Phys.Rev.**D45** (1992) 3206;  
Markus A. Luty and Rabindra N. Mohapatra, Phys.Lett.**B396** (1997) 161 [hep-ph/9611343];  
K. Hagiwara, K. Hikasa and M. Tanabashi, Phys.Rev.**D66** (2002) 010001; Phys.Lett.**B592** (2004) 1.
- [6] For a review and additional references, see R.R. Volkas and G.C. Joshi, Phys. Rep. **159** (1988) 303.
- [7] H. Harari and N. Seiberg, Phys.Lett. **B98** (1981) 269;  
M.E. Peskin, in *proceedings of the 1981 International Symposium on Lepton and Photon Interaction at High Energy*, W.Pfeil, ed., p880 (Bonn, 1981);  
L. Lyons, Oxford University Publication 52/82 (June 1982);  
G. 't Hooft, in Recent Developements in Gauge Theories;  
G. 't Hooft *et al.*, ads. (Plenum Press, New York,1980).
- [8] F. Boudjema, A. Djouadi, and J. Kneur, Z. Phys. **C57** (1993) 425;  
K. Hagiwara, D. Zeppenfeld and S. Komamiya, Z. Phys. **C29**, 115 (1985);  
N. Cabibbo, L. Maiani and Y. Srivastava, Phys. Lett. **B139**, 459 (1984).
- [9] U. Baur, M. Spira, and P. Zerwas, Phys. Rev. **D42** (1990) 815;  
J.Kuhn and P. Zerwas, Phys.Lett. **B147** (1984) 189.

- [10] ALEPH Collaboration, Phys. Lett. **B385** (1996) 445;  
 OPAL Collab., Eur. Phys. J. **C14** (2000) 73;  
 L3 Collab., Phys. Lett. **B568** (2003) 23;  
 DELPHI Collaboration, Eur.Phys. J. **C 8** (1999) 41; Eur. Phys. J. **C46** (2006) 277.
- [11] H1 Collaboration, Phys.Lett.**B678** (2009)335; Phys.Lett.**B666** (2008) 131; Eur. Phys. J. **C 17** (2000) 567;  
 ZEUS Collaboration S. Chekanov *et al.*, Phys. Lett. B **549** (2002) 32.
- [12] CDF Collaboration, Phys. Rev. Lett. **94** (2005) 101802; Phys. Rev. Lett. **97** (2006) 191802;  
 D0 Collaboration, Phys. Rev. **D73** (2006) 111102; Phys. Rev. **D77** (2008) 091102.
- [13] CMS Collaboration, Phys.Lett. **B704** (2011) 143.
- [14] ATLAS Collaboration, Phys.Rev. **D85** (2012) 072003.
- [15] J.L. Diaz and O.A. Sampayo, Phys.Rev. **D49** (1994) R2149.
- [16] J.I. Aranda, R. Martinez and O.A. Sampayo, Phys.Rev. **D62** (2000) 013010.
- [17] Swapan Majhi, Phys.Rev. **D88** (2013) 074028.
- [18] D. Choudhury, S. Majhi and V. Ravindran, JHEP **0601** (2006) 027.
- [19] P. Mathews, V. Ravindran, K. Sridhar and W.L. van Neerven, Nucl. Phys. **B713** (2005) 333 [hep-ph/0411018].
- [20] G. Altarelli, R.K.Ellis and G. Martinelli, Nucl. Phys. **B157** (1979) 461;  
 B.Humpert and W.L. van Neerven, Phys. Lett. **B84** (1979) 327; [Errat. **B85** (1979) 471];  
 ibid. **B89** (1979) 69; Nucl. Phys. **B 184** (1981) 225;  
 J.Kubar, M. le Bellac, J.L.Meunier and G. Plaut, Nucl. Phys. **B175** (1980) 251;  
 P. Aurenche and P. Chiapetta, Z.Phys. **C34** (1987) 201;  
 P.J.Sutton, A.D.Martin, R.G. Roberts W.J.Stirling, Phys. Rev. **D45** (1992) 2349;  
 P.J. Rijken and W.L. van Neerven, Phys. Rev. **D51** (1995) 44 [hep-ph/9408366].
- [21] J. Pumplin, D.R. Stump, J. Huston, H.L. Lai, Pavel M. Nadolsky and W.K. Tung, JHEP **0207** (2002) 012.
- [22] A.D. Martin, W.J. Stirling, R.S. Thorne and G. Watt, Eur. Phys. J. **C63** (2009) 189285.
- [23] O.J.P. Eboli, S.M. Lietti and P. Mathews, Phys.Rev. **D65** (2002) 075003.
- [24] S. C. Inan, Phys.Rev. **D81** (2010) 115002.